INTERNATIONAL JOURNAL OF PRECISION ENGINEERING AND MANUFACTURING Vol. 17, No. 1, pp. 11-17 JANUARY 2016 / 11
DOI: 10.1007/s12541-016-0002-3 ISSN 2234-7593 (Print) / ISSN 2005-4602 (Online)

Sensorless Collision Detection based on Friction Model for a Robot Manipulator

Sang-Duck Lee[1] and Jae-Bok Song[1,#]

1 School of Mechanical Engineering, Korea University, 145, Anam-ro, Seongbuk-gu, Seoul, 02841, South Korea
Corresponding Author / E-mail: jbsong@korea.ac.kr, TEL: +82-2-3290-3363, FAX: +82-2-3290-3757

KEYWORDS: Sensorless collision detection, Friction torque model, Collision safety

The importance of human-robot collision safety has been increasing recently due to the introduction of collaborative robots. However, conventional collision detection methods usually require additional sensors such as skin sensors, joint torque sensors, and acceleration sensors, which are impractical to implement due to their high cost. To address this problem, in this study we propose a collision detection method using only a manipulator's encoder without any extra sensors. In the proposed scheme, the external torque due to collision is estimated using a generalized momentum-based observer and a friction torque model in the harmonic drive developed for a robot that is conducting position control. The performance of the proposed collision detection method was evaluated using a 6 DOF industrial manipulator. The experimental results show that collision can be reliably detected without any extra sensors for any type of robot manipulator.

Manuscript received: January 15, 2015 / Revised: October 11, 2015 / Accepted: November 6, 2015

1. Introduction

In many industries, collaborations between humans and robots have become increasingly important. However, collaborative robots can harm the humans with whom they share the workspace due to human errors or malfunctions. For these reasons, the importance of human-robot collision safety has been increasing recently. Several solutions have been proposed to ensure human-robot collision safety, such as the installation of a mechanism that can absorb impact forces,[1] the use of a vision sensor to avoid collisions,[2] and the design and control of manipulators based on collision analysis and safety evaluation.[3,4] Although these solutions have been used to improve collision safety, there are a number of disadvantages with each. Adding additional mechanisms is a rather passive solution, which lacks flexibility and increases the size and complexity of the robot; vision sensors have limitations such as blind spots and heavy computational load in dynamic environments, while merely using safety evaluations to design and control systems requires a tradeoff between task performance and collision safety. On the other hand, improvement of collision safety through collision detection, in which the robot can minimize an impact by performing an appropriate reaction, has several advantages: it requires no installation of extra mechanisms, it has relatively high reliability, and it does not affect task performance. A number of studies have therefore been carried out on collision detection.

The use of a skin sensor for collision detection was demonstrated.[5] Several studies have been conducted on human-robot collision detection using the joint torque sensors embedded in the manipulator for torque control. Collision detection algorithms using a disturbance observer have also been proposed.[6] Recently, research in the area of human-robot collision detection has focused on collision detection using generalized momentum instead of acceleration.[7,8] However, these conventional collision detection methods are sensor based methods, and the use of sensors may increase the cost of a robot significantly and additionally require a design change. Moreover, it is impossible to apply conventional collision detection methods to most manipulators used in industrial fields because they are not equipped with such sensors. Therefore, there is a need to develop a collision detection method that can detect collisions without the use of extra sensors.

In this study, we propose a collision detection method that does not require any extra sensors such as F/T sensors and accelerometers. We observe the external torque that is applied to the joints of a manipulator by monitoring the motor current and the dynamic model of the manipulator. We identify a friction model of manipulator joints based on the least squares technique. The proposed collision detection method was verified experimentally with a 6 degrees of freedom (DOF) industrial manipulator, and the experimental results show that

collisions can be detected reliably using the proposed collision detection method.

The two main features of the proposed collision detection method can be summarized as follows: 1) the proposed collision detection method can be applied to any manipulator ranging from industrial manipulators to service robots because it does not require extra sensors and 2) to estimate the friction model of a joint without sensors, we employ an observer which does not require linearization of the friction torques or an adaptation scheme.

The remainder of this paper is organized as follows. In section 2, the proposed sensorless collision detection scheme will be overviewed. The developed method for friction model identification is introduced in section 3. Section 4 presents an experimental verification, and section 5 presents our conclusion.

2. Sensorless Collision Detection

When a human-robot collision occurs, external torque is applied to each joint of a manipulator, so collisions can be detected by observing this external torque. The external torque can be calculated from a dynamic model of the manipulator, and an equation of motion of the manipulator including external torque can be written by

$$M(q)\ddot{q}+C(q,\dot{q})\dot{q}+g(q)=\tau_j-\tau_{ext} \tag{1}$$

where $M(q)$ is the inertia matrix, $C(q,\ \dot{q}\ )$ is the matrix containing Coriolis and centrifugal terms, and $g(q)$ is the gravity vector. The variables q, $\dot{q}$, and $\ddot{q}$ are the joint position, velocity, and acceleration vector, τ_j is the joint torque vector applied to each link of the manipulator, and τ_{ext} is the external torque vector generated by collision. From Eq. (1), τ_{ext} can be presented as follows:

$$\tau_{ext}=\tau_j-(M(q)\ddot{q}+C(q,\dot{q})\dot{q}+g(q)) \tag{2}$$

In Eq. (2), the dynamic parameters can be estimated from the CAD files of a manipulator, and $q,\ \dot{q}$ can be measured by the encoders. However, τ_j and $\ddot{q}$ cannot be directly measured without the use of extra sensors such as joint torque sensors and accelerometers.

To solve Eq. (2) without the use of sensors, we calculate the joint torque τ_j based on the motor input current, i and joint friction torque, τ_f. The relationship between i and τ_f can be obtained by investigating the power transmission of the joint. In general, the joint of a manipulator is equipped with an actuator (e.g., AC servo motor) and a speed reducer (e.g., harmonic drive); the typical components and power transmissions of such a joint are shown in Fig. 1. Since the motor torque τ_m is proportional to the motor current i, τ_m can be expressed by

$$\tau_m=K_T i \tag{3}$$

where K_T is the torque constant that defines the relationship between τ_m and i, which is provided by the motor manufacturer. Note that the torques due to the internal friction and rotor inertia of the motor are assumed to be negligible.

Assuming no power is lost in the joint due to the friction torque, the

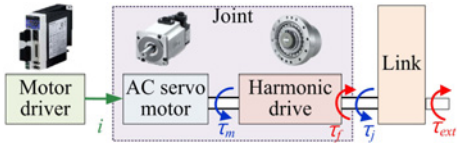

Fig. 1 Power transmission of manipulator joints

output joint torque is $\tau_a=\rho\tau_m$, where ρ is the speed reduction ratio. However, some of $\rho\tau_m$ is consumed by the friction of the harmonic drive, so the actual joint torque τ_j can be given by

$$\tau_j=\rho\tau_m-\tau_f=\rho K_T i-\tau_f \tag{4}$$

where τ_f is the friction torque vector in the harmonic drive. Substituting Eq. (4) into Eq. (2) yields

$$\tau_{ext}+\tau_f=\rho K_T i-(M(q)\ddot{q}+C(q,\dot{q})\dot{q}+g(q)) \tag{5}$$

Thus, we can calculate τ_{ext} by using i and τ_f without measuring τ_j.

To solve Eq. (5) without the use of an accelerometer for the measurement of $\ddot{q}$, we adopted an observer that is designed based on the low-pass filter and the generalized momentum expressed by

$$p=M(q)\dot{q} \tag{6}$$

Since $M(q)$ is a symmetric matrix, we can define the skew-symmetric matrix $N(q,\dot{q})=\dot{M}(q)-2C(q,\dot{q})$, and we can solve for $M(q)$.[9]

$$\dot{M}(q)=C^T(q,\dot{q})+C(q,\dot{q}) \tag{7}$$

Using Eq. (7), the time-derivative of p can be expressed as

$$\dot{p}=M(q)\ddot{q}+\dot{M}(q)\dot{q}=M(q)\ddot{q}+\{C^T(q,\dot{q})+C(q,\dot{q})\}\dot{q} \tag{8}$$

Substituting Eq. (5) into (8) gives

$$\begin{aligned}\dot{p}&=\rho K_T i+C^T(q,\dot{q})\dot{q}-g(q)-(\tau_{ext}+\tau_f)\\&=\rho K_T i+C^T(q,\dot{q})\dot{q}-g(q)-r\end{aligned} \tag{9}$$

where $r=\tau_{ext}+\tau_f$ is the sum of the unknown terms that should be observed.

Now, consider a first-order low-pass filter written by

$$\frac{\hat{r}(s)}{r(s)}=\frac{K}{s+K} \tag{10}$$

where $\hat{r}(s)$ is the filtered value of r and K is the cutoff frequency of this filter. An interesting feature of this low-pass filter is that the effect of electrical noise from the sensors can be minimized, while achieving a reasonable response time by setting an appropriate value for K.[8] Thus, we can estimate r based on $\hat{r}(s)$ if the control period is sufficiently fast. By taking the inverse Laplace transform of Eq. (10), we get

$$\dot{\hat{r}}=K(r-\hat{r}) \tag{11}$$

Assuming a moderate control period, the forward difference of $\hat{r}(s)$ is

represented in discrete time by

$$\frac{\hat{r}(k+1)-\hat{r}(k)}{T} = K[r(k)-\hat{r}(k)] \tag{12}$$

where k is the discrete-time index and T is the sampling period. Taking the summation on both sides of Eq. (12) yields

$$\sum_{k=0}^{n}[\hat{r}(k+1)-\hat{r}(k)] = KT\sum_{k=0}^{n}[r(k)-\hat{r}(k)] \tag{13}$$

where n is the upper limit of summation. Assuming the zero initial condition (i.e., $\hat{r}(0) = 0$), expansion of the left-hand side yields

$$\hat{r}(n+1) = KT\sum_{k=0}^{n}[r(k)-\hat{r}(k)] \tag{14}$$

Substitution of the discretized version of Eq. (9) into Eq. (14) gives

$$\hat{r}(n+1) = KT\sum_{k=0}^{n}[\rho K_T i(k)+C^T(k)\dot{q}(k)-g(k)-\dot{p}(k)-\hat{r}(k)] \tag{15}$$

The backward difference of p is given by $\dot{p}(k) = (p(k)-p(k-1))/T$ with the assumption of $p(0) = 0$. Then, Eq. (15) can be represented by

$$\begin{aligned}&\hat{r}(n+1)\\ &= KT\left[\sum\{\rho K_T i(k)+C^T(k)\dot{q}(k)-g(k)-\hat{r}(k)\}\right]-K\left[\sum_{k=0}^{n}\{p(k)-p(k-1)\}\right]\\ &= KT\left[\sum\{\rho K_T i(k)+C^T(k)\dot{q}(k)-g(k)-\hat{r}(k)\}\right]-Kp(n)\end{aligned} \tag{16}$$

Note that $\dot{q}(k)$ can be estimated from the encoder signal. From Eq. (16), the variable r can be observed without the use of extra sensors by assuming $r \approx \hat{r}$.

Because $r = \tau_{ext} + \tau_f$, we can estimate τ_{ext} from r if τ_f is given. However, the use of the sensors such as joint torque sensors or a force/torque sensor to measure τ_f is limited due to the high cost of such sensors. Thus, we employ the friction model of the manipulator joint and its identification scheme to estimate τ_f.

3. Friction Model of a Joint

3.1 Friction torque model

The general friction model of a mechanical system has three components: 1) static friction, τ_s, which represents the force necessary to initiate the motion from rest; 2) Coulomb friction (or kinetic friction), τ_c, which depends only on the sign of the velocity; and 3) viscous friction, τ_v, which is a function of the relative velocity between contacting surfaces. As a result, the friction torque model of the manipulator joint can be described by

$$\tau_f = \begin{cases} \tau_h, & \text{if } \dot{q}=0 \text{ and } |\tau_h|<\tau_s \\ \tau_s\text{sgn}(\tau_h), & \text{if } \dot{q}=0 \text{ and } |\tau_h|\geq\tau_s \\ \tau_c\text{sgn}(\dot{q})+\tau_v(\dot{q}), & \text{if } \dot{q}\neq 0 \end{cases} \tag{17a}$$

where $\tau_v(\dot{q}) = \beta_1\dot{q}^3+\beta_2\dot{q}^2+\beta_3\dot{q}$ (17b)

where τ_h is the torque acting on the interface between the contacting surfaces of the components in the harmonic drive, and β_1, β_2, and β_3 are the coefficients of the viscous friction $\tau_v(\dot{q})$, which is assumed to be expressed by a third-order function of $\dot{q}$ since the slope of τ_v decreases with increasing $\dot{q}$.[10] Based on this friction model, τ_f can be expressed in terms of $\dot{q}$ as shown in Fig. 2(a), which illustrates two different friction regions: the stick region where $\dot{q}=0$ and the slip region where $\dot{q}\neq 0$. The friction torque in the transition from the stick to the slip region is τ_s, and that from the slip to the stick region is $\pm\tau_c$.

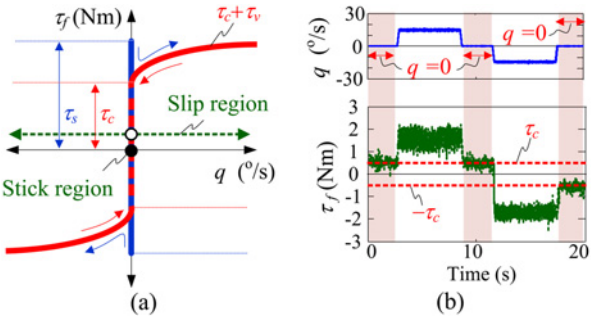

Fig. 2 Friction torque of the joint: (a) two friction regions and (b) estimated friction torque with time (experiment)

Fig. 2(b) shows the joint velocity $\dot{q}$ and estimated friction torque $\hat{\tau}_f$ with time. The experimental conditions will be detailed in Sec. 4. In general, the friction torque of an object at rest (i.e., τ_h) depends on the torque applied to the object; however, in the case of a manipulator joint, this torque is $\pm\tau_c$ as shown in Fig. 2(b). This is because the manipulator is position-controlled and thus the torque applied to the harmonic drive is maintained at a certain value that makes the joint reach the desired position. Therefore, τ_h becomes $\pm\tau_c$ in the transition from the slip to the stick region and its value is maintained in the stick region.

Consequently, the friction model for sensorless collision detection can be described by

$$\tau_f = \begin{cases} \tau_c\text{sgn}(\tau_h), & \text{if } |\dot{q}|<\varepsilon \text{ and } \dot{q}_d=0 \\ \tau_s\text{sgn}(\tau_h), & \text{if } |\dot{q}|<\varepsilon \text{ and } \dot{q}_d\neq 0 \\ \tau_c\text{sgn}(\dot{q})+\tau_v(\dot{q}), & \text{if } |\dot{q}|\geq\varepsilon \end{cases} \tag{18}$$

where ε is the maximum magnitude of the electrical noise of $\dot{q}$ and thus $|\dot{q}| < \varepsilon$ means the joint can be regarded to be at rest. Note that e is employed to avoid the chattering problem. Since the static friction t_s in Eq. (17) is unknown before it is identified, we use the quantity $\dot{q}_d$ to check whether or not the joint is in the transition from the stick to the slip region because $\dot{q}$ follows $\dot{q}_d$. That is, the joint is on the verge of rotating if it is currently at rest, but $\dot{q}_d\neq 0$. The Dahl and the Stribeck effects are not considered in our friction model because we are interested in covering the friction torque over the wide range of joint velocity with a simple friction model for collision detection.

3.2 Friction model identification

If the parameters of the friction model such as τ_c and τ_s are given, τ_f can be obtained from Eq. (18) using $\dot{q}$, which is measured by the encoder. However, it is very difficult to derive such parameters theoretically, so an identification scheme is required for their estimation. If an online identification scheme is employed for collision detection,

a friction model can be identified to compensate for the external torque generated by the collision; however, this approach can lead to inaccurate identification and errors in the observed external torques. Thus, an offline identification scheme is a more appropriate approach for collision detection, and we identify the friction model using the least squares technique, which is a typical and widely used technique for the offline identification method.

To identify the unknown parameters in Eq. (18), we rearrange this equation to the following regressor form

$$\tau_f = W\theta \tag{19}$$

where

$$W = [w_1 \mathrm{sgn}(\tau_h) + w_3 \mathrm{sgn}(\dot{q}) \quad w_2 \mathrm{sgn}(\tau_h) \quad w_3\dot{q} \quad w_3\dot{q}^2 \quad w_3\dot{q}] \tag{20a}$$

$$\theta = [\tau_c \quad \tau_s \quad \beta_1 \quad \beta_2 \quad \beta_3]^T \tag{20b}$$

where W is the regressor matrix that is a function of $\dot{q}$ and τ_h, and θ is the vector of unknown parameters. w_1, w_2, and w_3 are the weighting factors that indicate the friction regions and transition as follows:

$$w_1 = \begin{cases} 1, & \text{if } |\dot{q}| < \varepsilon \text{ and } \dot{q}_d = 0 \\ 0, & otherwise \end{cases},$$

$$w_2 = \begin{cases} 1, & \text{if } |\dot{q}| < \varepsilon \text{ and } \dot{q}_d \neq 0 \\ 0, & otherwise \end{cases} \tag{21}$$

$$w_3 = \begin{cases} 1, & \text{if } |\dot{q}| \geq \varepsilon \\ 0, & otherwise \end{cases}$$

If τ_f and W are obtained at given instants along a certain trajectory, Eq. (19) can be represented as

$$\overline{\tau}_f = \begin{bmatrix} \tau_{f1} \\ \cdots \\ \tau_{fi} \\ \cdots \\ \tau_{fn} \end{bmatrix} = \begin{bmatrix} W_1 \\ \cdots \\ W_i \\ \cdots \\ W_n \end{bmatrix} \theta = \overline{W}\theta \tag{22}$$

where τ_{fi} and W_i are τ_f and W at the time instant i, and $\overline{\tau}_f$ and $\overline{W}$ are the sets containing many corresponding values of τ_{fi} and W_i. If the size of these sets is large enough, θ can be identified using a least-squares technique as follows

$$\theta = \overline{W}^{+}\overline{\tau}_f \tag{23}$$

where $\overline{W}^{+}$ is the pseudo-inverse matrix of $\overline{W}$. As a result, the friction torque can be estimated using the friction model by substituting the identified parameters of θ into Eq. (18).

3.3 Friction torque observer

While friction torque is required to identify θ in Eq. (23), using the sensors for its measurement is an impractical solution to sensorless collision detection, as mentioned previously. This problem can be dealt with by adopting a friction torque observer. However, its applicability is limited since conventional friction torque observers are based on the linearization of friction torque and the adaptation of the observer.[11] Thus, we employ a new friction torque observer based on the observer in Eq. (16).

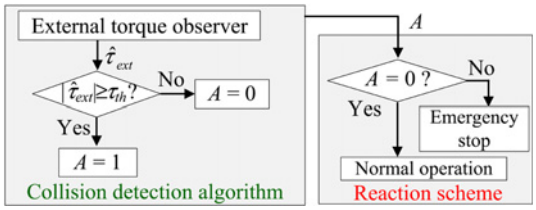

Fig. 3 Flowchart of collision detection algorithm

Since $r = \tau_{ext} + \tau_f$, r is equal to τ_f if no collision occurs (i.e., $\tau_{ext} = 0$). In this case, the estimate $\hat{r}$ can be used to estimate τ_f as follows:

$$\hat{\tau}_f(n+1) = KT\left[\sum_{k=0}^{n}\{\rho K_T i(k) + C^T(k)\dot{q}(k) - g(k) - \hat{r}(k)\}\right] - Kp(n) \tag{24}$$

where $\hat{\tau}_f$ is the estimate of τ_f. If the estimator error is sufficiently small, we can assume $\hat{\tau}_f = \tau_f$, and thus $\overline{\tau}_f$ can be calculated based on $\hat{\tau}_f$. τ_h in $\overline{W}$ can also be calculated using $\hat{\tau}_f$ because the joint is force balanced in the stick region and thus $\tau_h = \tau_f$. Therefore, θ can be identified by substituting calculated $\overline{\tau}_f$ and $\overline{W}$ into Eq. (23).

The friction force τ_f can be calculated without the use of any sensors by substituting the identified parameters in θ into the friction model in Eq. (15). Then,

$$\tau_{ext} = \hat{r} - \tau_f \tag{25}$$

where $\hat{\tau}_{ext}$ is the estimate of τ_{ext}. Note that $\hat{\tau}_f$ in Eq. (24) cannot be used to replace τ_f in Eq. (25), because $\tau_{ext} \neq 0$ when a collision occurs, and this identification scheme is conducted in controlled conditions.

Ideally, $\hat{\tau}_{ext}$ approaches zero when no collision exists, but this condition rarely happens due to the uncertainty in the dynamic model of the manipulator and friction torque model. Therefore, collisions should be detected by comparing the absolute value of $\hat{\tau}_{ext}$ with a threshold τ_{th} that is experimentally determined. Fig. 3 indicates the flowchart of the collision detection algorithm. In this flowchart, A is an indicator of collision detection, and it is determined by the comparison of τ_{ext} with τ_{th}, and A can be used to determine the reaction scheme of the entire control system (e.g., emergency stop after collision detection).

4. Experiments and Discussion

The experimental verification of the proposed collision detection method was conducted using the 6 DOF industrial manipulator shown in Fig. 4. This manipulator was developed in our laboratory. It has a reachable distance of 1044 mm and weighs about 33 kg with a payload of 6 kg. For the operation of the AC servo motor at each joint of this manipulator, a motion controller installed in a PC communicates commands to the motor drive. Windows is used as the main operating system, thus real-time operation is confirmed using an external timer, and the control period is 1 ms.

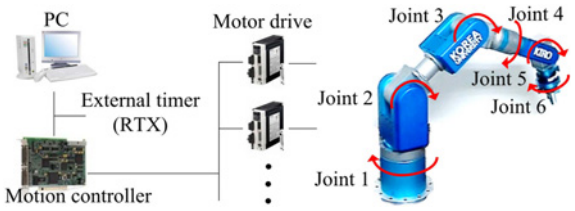

Fig. 4 Experimental setup with 6 DOF industrial manipulator

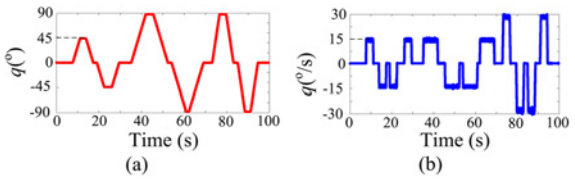

Fig. 5 Trajectory for friction model identification: (a) position and (b) velocity

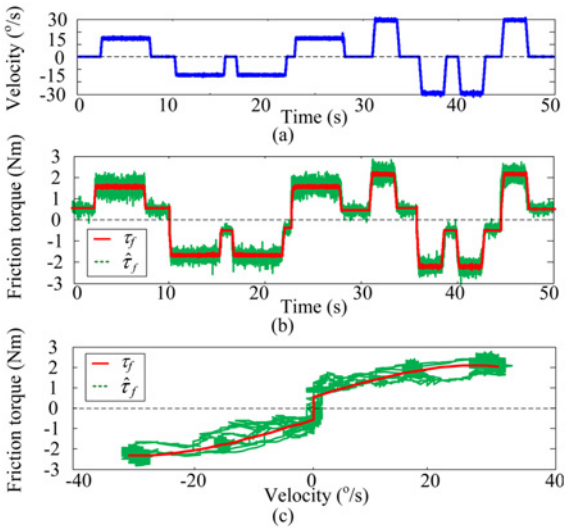

Fig. 6 Experimental verification of friction model: (a) experimental conditions, (b) friction torque with time, and (c) friction torque with velocity

4.1 Validation of friction torque model

As can be seen from Eq. (25), $\hat{\tau}_{ext}$ is calculated using the friction model. We therefore conduct experimental validation of the reliability of this friction model by comparing τ_f, which is calculated with the friction model, with $\hat{\tau}_f$ prior to the verification of collision detection performance. However, as can be deduced from Eq. (24), the assumption of $\hat{\tau}_f = \tau_f$ is not satisfied if some errors exist in the dynamic model of a manipulator. Thus, in such a case, it is impossible to verify the reliability of the friction model through comparison between $\hat{\tau}_f$ and τ_f. On the other hand, $\hat{\tau}_f$ at joint 6 is free from this type of error because joint 6 is not attached to the link when the tool is not attached to the end-effector. Therefore, the verification of the friction model is carried out based on joint 6 to investigate the features of the friction torque more clearly.

To compare τ_f with $\hat{\tau}_f$, the friction model should first be identified and Fig. 5 shows the condition for this identification. The tool on the end-effector was removed, and $\overline{W}$ and $\overline{\tau}_f$ were obtained along the trajectory shown in Fig. 5. By substituting the obtained data set into Eq. (23), we can calculate θ and identify the friction model.

An experiment was conducted to compare τ_f (based on the identified friction model) with $\hat{\tau}_f$. Fig. 6(a) shows the velocity profile of joint 6, and Figs. 6(b) and 6(c) show the experimental results. As seen from Fig. 6, τ_f retains its value when q=0, and this result is consistent with the previously explained features of friction torque. In addition, τ_f and τ_f show good agreement, which means that the proposed friction model and its identification method work very well; we therefore conclude that τ_{ext} can be obtained using Eq. (25) for sensorless collision detection.

4.2 Sensorless collision detection

To verify the applicability of the proposed collision detection method, an experiment was conducted in which the manipulator collides with a human. Fig. 7 shows the experimental conditions, in which the manipulator moved from the initial pose shown in Fig. 7(a) to the target pose shown in Fig. 7(b) using the proposed collision detection method. In this operation, joints 2, 3, and 5 were rotated 30°, the other axes were rotated 10°, and the velocity of every joint was 30°/s. Two experiments were conducted: the first with no collision and the second with a collision with a human as shown in Fig. 7(c). τ_{ext} and collision force F_c (which was measured by the F/T sensor mounted at the manipulator), were acquired during these experiments.

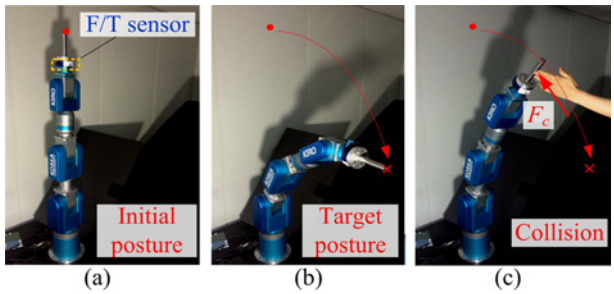

Fig. 7 Experimental verification of collision detection performance: (a) initial posture, (b) target posture, and (c) collision with human

Figs. 8(a) and 8(b) show τ_{ext} at joint 1 and F_c during the experiment shown in Fig. 7. Fig. 8(a) shows that τ_{ext} exceeded the threshold τ_{th}, which was set to 8 Nm when a collision occurred. This means that collisions can be detected based on whether or not τ_{ext} exceeds τ_{th}. In Fig. 8(b), F_c increased rapidly when a collision occurred, and decreased after it reached its peak value of 48 N because the manipulator immediately stopped when the collision was detected. Without the proposed collision detection method, the manipulator would have continued to apply the collision force to the human because the position control scheme tries to reach a target position even if a collision occurs. These experiments show that the manipulator can detect collisions without the use of any extra sensors, and collision safety can be ensured by applying the proposed collision detection method.

To validate the external torque estimate τ_{ext}, we investigate how

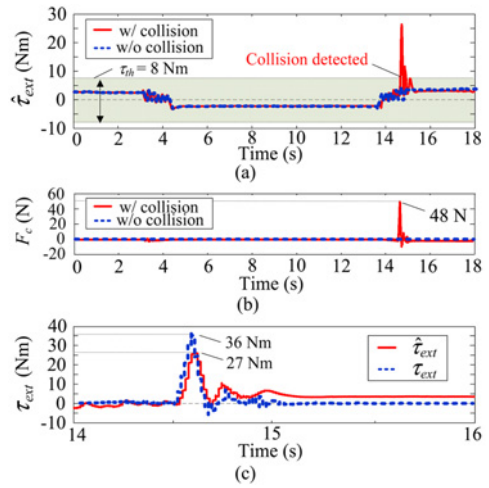

Fig. 8 Experimental results: (a) τ_{ext}, (b) F_c, and (c) validation of τ_{ext}

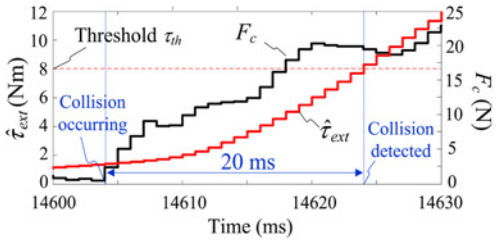

Fig. 9 Close-up view of τ_{ext} and time delay of collision detection

close it is to the actual external torque τ_{ext}. Fig. 8(c) shows the results, and τ_{ext} in Fig. 8(c) is the close-up view of Fig. 8(a). τ_{ext} in Fig. 8(c) is computed based on F_c and inverse statics (i.e. $\tau_{ext} = J^T F_c$), and the observed joint was joint 1. As shown in Fig. 8(c), the shapes of the graphs for τ_{ext} and τ_{ext} are similar to each other, and the difference between the peak values of τ_{ext} and τ_{ext} is smaller than the threshold torque τ_{th} (8 Nm). Therefore, we conclude that the external torque estimate t_{ext} is reasonably close to the actual value.

The time delay between the collision and the detection is also important for the practical use of the proposed collision detection method. Thus, based on the experiment shown in Fig. 7, this delay was evaluated by comparing the F/T sensor data. Fig. 9 shows a close-up view of τ_{ext} and F_c shown in Fig. 8. We can estimate the moment of collision from the sudden increase in F_c in Fig. 9 and the time required for the detection by comparing τ_{ext} and τ_{th}. In the ideal case of $\tau_{th} = 0$, a fault can be detected within 1 ms, which corresponds to the control period of the system. However, in the case of τ_{th} = 8 Nm, in consideration of the uncertainties in the dynamic model of the manipulator including the friction model, the manipulator can detect a collision within 20~21 ms. These delays are inevitable, but can be improved by using a more accurate model.

5. Conclusions

A sensorless collision detection algorithm based on the external torque observer and friction model identification was proposed in this study. The proposed collision detection method is verified experimentally with a 6 DOF industrial manipulator, and the following conclusions were drawn.

1) Because the proposed collision detection method does not require extra sensors, it can be applied to existing manipulators without a change of design and/or additional mechanisms. Therefore, it is a practical solution to ensure the collision safety of various manipulators.

2) Collisions are detected based on the external torque generated by the collision. Therefore, the manipulator can detect collisions more sensitively compared to the simple limitation of the motor current, which can be consumed by the friction torque and motion control of the manipulator.

3) The friction torque observer is established without the linearization of the friction torque and adaptation of the observer. Therefore, this approach provides new insights into how to estimate the friction torque of various mechanical systems without sensors.

ACKNOWLEDGEMENT

This research was supported by Basic Science Research Program through the NRF of Korea funded by the MSIP (No. 2007-0056094) and the MOTIE under the Industrial Foundation Technology Development Program supervised by the KEIT (No. 10048980).

REFERENCES

1. Choi, D.-E., Lee, W., Hong, S. H., Kang, S.-C., Lee, H., and Cho, C.-H., "Design of Safe Joint with Variable Threshold Torque," Int. J. Precis. Eng. Manuf., Vol. 15, No. 12, pp. 2507-2512, 2014.

2. Flacco, F., Kröger, T., De Luca, A., and Khatib, O., "A Depth Space Approach to Human-Robot Collision Avoidance," Proc. of IEEE International Conference on Robotics and Automation (ICRA), pp. 338-345, 2012.

3. Lee, S.-D., Kim, B.-S., and Song, J.-B., "Human–Robot Collision Model with Effective Mass and Manipulability for Design of a Spatial Manipulator," Advanced Robotics, Vol. 27, No. 3, pp. 189-198, 2013.

4. Haddadin, S., Haddadin, S., Khoury, A., Rokahr, T., Parusel, S., et al., "A Truly Safely Moving Robot has to Know what Injury it May Cause," Proc. of IEEE/RSJ International Conference on Intelligent Robots and Systems (IROS), pp. 5406-5413, 2012.

5. Ulmen, J. and Cutkosky, M., "A Robust, Low-Cost and Low-Noise Artificial Skin for Human-Friendly Robots," Proc. of IEEE International Conference on Robotics and Automation (ICRA), pp. 4836-4841, 2010.

6. Dixon, W. E., Walker, L. D., Dawson, D. M., and Hartranft, J. P., "Fault Detection for Robot Manipulators with Parametric Uncertainty: A Prediction-Error-based Approach," IEEE Transactions on Robotics and Automation, Vol. 16, No. 6, pp. 689-

699, 2000.

7. De Luca, A. D. and Mattone, R., "Actuator Failure Detection and Isolation using Generalized Momenta," Proc. of IEEE International Conference on Robotics and Automation, Vol. 1, pp. 634-639, 2003.
8. Haddadin, S., Albu-Schäffer, A., De Luca, A., and Hirzinger, G., "Collision Detection and Reaction: A Contribution to Safe Physical Human-Robot Interaction," Proc. of IEEE/RSJ International Conference on Intelligent Robots and Systems, pp. 3356-3363, 2008.
9. Sciavicco, L. and Siciliano, B., "Modelling and Control of Robot Manipulators," Springer, 2nd Ed., pp. 140-143, 2000.
10. Seyfferth, W., Maghzal, A., and Angeles, J., "Nonlinear Modeling and Parameter Identification of Harmonic Drive Robotic Transmissions," Proc. of IEEE International Conference on Robotics and Automation, Vol. 3, pp. 3027-3032, 1995.
11. Le Tien, L., Albu-Schäffer, A., De Luca, A., and Hirzinger, G., "Friction Observer and Compensation for Control of Robots with Joint Torque Measurement," Proc. of IEEE/RSJ International Conference on Intelligent Robots and Systems, pp. 3789-3795, 2008.